Applicability of FTIR and Raman Spectroscopic Methods to the Study of Paper–ink Interactions in Digital Prints

Katri Vikman▲ and Katja Sipi

Helsinki University of Technology, Laboratory of Media Technology, Espoo, Finland

Vibrational spectroscopic methods are widely used in analyzing materials both in xy- and z-directions. The need to gain a deeper understanding of the print durability, especially the light fastness of ink jet prints and toner adhesion mechanisms in electrophotography, calls for analytical techniques that are capable of detecting both the physical and chemical state of prints. The sample sets used to study the applicability of various FTIR and Raman techniques to analyzing paper–ink interactions included ink jet prints with the light exposure time as a variable, and electrophotographic prints fixed at different conditions. Because of their versatility and ability to detect features from inks, toners and papers, Raman and FTIR spectroscopy proved to be suitable for studying paper–ink interactions. In addition, these methods also detected changes in the spectra due to light exposure and fixing. In examining ink jet prints on coated papers, FTIR-ATR, confocal Raman and UV Resonance Raman spectroscopy (UVRRS) turned out to be the most suitable methods for studying the light fastness of the prints. In studying the adhesion of electrophotographic prints, various FTIR methods seemed to be particularly useful because of their ability to detect hydrogen bonding.

Journal of Imaging Science and Technology 47: 139-148 (2003)

Introduction

Traditional optical print quality measurement methods do not yield enough information for deducing of paper–ink interactions occurring in digital prints. For this reason, several other analytical methods have been used in studying papers and prints. The physical state of prints, characterized by aggregation and penetration of inks and toners, has been examined with various microscopic methods, often combined with thin-cuts of paper. These include optical microscopy,[1] atomic force microscopy (AFM),[2] and transmission (TEM) and reflection (REM) electron microscopy.[3] The disadvantage of these methods is that they do not give direct information on the chemical structure of the interface. In addition, the use of resin in conventional microtoming methods may be problematic in studying electrophotographic prints, since resin is also the main component of the toners.

The chemical state of prints has been studied using a myriad of methods. Paper chromatography[4] and thin-layer chromatography[5] have been used in particular to examine ink jet prints. Their drawbacks are the excessive amount of ink solvent present compared to an actual ink jet printing situation and the impossibility of studying real prints. The use of thermal analysis,[6] and absorbance and zeta potential measurements[7] in interaction studies in ink jet printing has also been reported. Electron spectroscopy for chemical analysis (ESCA) has been utilized in studying both the chemical structure of the paper surface and its print properties, including toner adhesion. It gives information on the chemical structure of the material, such as the electronic structure and bonding of single atoms, but is unable to detect certain chemical groups that are essential in paper–ink interactions, like OH. In some cases, especially in ink jet printing, the extreme surface sensitivity of ESCA may further complicate the interaction studies.[8]

Vibrational spectroscopy, IR and Raman spectroscopy, enables a print to be studied "as is", and thus provides information on the actual paper–ink interactions. Other advantages include detailed molecular characterization, minimal demands for the sampling environment and ease of sampling preparation. So far these methods, especially Raman spectroscopy, have been relatively seldom used in paper and print analysis, mainly because of the fluorescence phenomenon in the Raman method. Novel excitation sources and FT devices have largely solved this problem.[9]

The present study is an extended version of two conference papers presented at IS&T's NIP16[10] and NIP17.[11] The objective of this work is to evaluate the applicability of various vibrational spectroscopic methods to paper–ink interaction studies in ink jet printing and electrophotography. In ink jet printing, the main concern is the light fastness of the printed image, whereas in electrophotography, the toner adhesion is of primary interest.

FTIR and Raman Spectroscopy in Print Studies

Although IR and Raman spectroscopy are both based on molecular vibrations, they are complementary meth-

Original manuscript received June 14, 2002

▲ IS&T Member

Email: katri.vikman@hut.fi, katja.sipi@hut.fi

ods, owing to their different mechanisms for transfer of energy from photons to exposed molecules. IR spectroscopy gives information on chemical groups containing highly polar bonds, or bonds whose dipole moment changes during vibration, as in the case of water. Conversely, Raman activity results if the polarizability of a molecule changes during vibration. This is true e.g. for symmetric covalent bonds, such as N=N.[12]

Both FTIR and Raman spectroscopy have been applied to studies of archeological findings, e.g., properties of historical papers have been examined using the attenuated total reflectance method (FTIR-ATR).[13] The ATR and DRIFT methods have been used in conjunction with multivariate statistical techniques in classifying of document papers.[14] Depth profiling of paper structures has been accomplished with photoacoustic FTIR spectroscopy (PAS) using the step-scan method. Analysis of FTIR-PAS results with a 2D correlation method has proved to be a suitable method for qualitative analysis of starch-based coating structures, because it gives information on the concentration profiles of the paper components.[15] However, accurate information on coating thickness can not be obtained with this method, because the detailed analysis requires information on the thermal diffusivities of the paper components. Analysis of the binder distribution in coating layers is another typical application of vibrational spectroscopy, which has been examined in various studies.[16–18] These investigations have utilized spectral information obtained with FTIR-ATR, confocal Raman and UV spectroscopic methods.

Vibrational spectroscopic methods have also proven to be applicable to studying colorants. For example, FTIR spectroscopy has been used to determine the mechanisms by which dye solutes specifically interact in an amorphous copolyester matrix[19] and with a variety of polymer structures.[20] FTIR measurements enabled determination of both the type and strength of interactions that occur between dyes containing hydroxyl groups and polymers containing functional groups. FTIR-PAS has also been utilized in identifying colorants and in measuring the light absorption of very thin ink layers.[21,22]

However, because of its sensitivity to aromatic structures[23] Raman spectroscopy is likely to be better applicable to ink studies than IR spectroscopy. Raman spectroscopy has been extensively applied to analyzing pigment structures and degradation of manuscripts.[24,25] In analyzing printed samples, fluorescence either from the paper or from the ink can markedly reduce the S/N-ratio of the spectrum. To overcome this problem, a Fourier-transform spectrometer with near-infrared excitation (NIR-FTR) and surface-enhanced resonance Raman scattering (SERRS) have been used in detection of ink jet dyes on paper surfaces.[26] With both methods, the detection of the colorant was possible, though, with NIR-FTR fluorescence still posed a problem, whereas the pre-treatment of the sample required for SERRS analysis prevented the prints from being studied as such.

Various vibrational spectroscopic methods have been widely used in polymer research both in surface studies[27,28] and in depth profiling,[29] which backs up their use in print analyses. Because of its capability of probing C-C and C-H bonds, Raman spectroscopy is particularly suitable for polymer studies. FTIR and Raman techniques have been used to examine the properties of polyesters containing diacetylene groups.[30] Raman was found to be a better technique for detecting the formation of polydiacetylene chains and for investigating the factors that affect the crosspolymerization. Photochemical curing and degradation of oil paints have also been studied with Raman spectroscopy.[31] Curing and degradation reactions of an unsaturated fatty acid ester binder were examined in terms of the properties of binder molecules and functional groups in them. FTIR with a micro-ATR set-up has also been utilized in analyzing paints.[32] The aging of paints was found to be manifested by the broadening of the absorption in the carbonyl region and the loss of intensity in the C=O and C-O stretching of phthalate ester.

Different FTIR detection methods have been used in polymeric coating research. Vibrational spectroscopic methods have been used to analyze surfaces of novel coatings.[33] The possibility of obtaining depth-profiling information with the ATR and PAS methods was found to be crucial in this kind of analysis. The use of PAS in polymeric coatings analysis has also been studied extensively.[34,35] For instance, it has been found that it is possible to separate complex processes occurring in the curing of alkyd coatings. Various stratification processes occurring in multicomponent coatings have also been identified.

Compositions of polymer blends have been examined extensively with vibrational spectroscopic methods. Different kinds of interactions and molecular bonds may be identified. For example, the ATR technique has been used to study the type and number of acid-base intermolecular interactions in certain polymer blends.[36] The fraction of acid-base bonded carbonyl groups and the degree of inter-association in polymer blends were established through quantitative curve-resolving analysis.

Experimental

Sample Preparation

To explore the applicability of FTIR and Raman spectroscopic techniques to studying ink jet and electrophotographic prints, sets of printed samples were prepared using light exposure time and fixing temperature, respectively, as controlled variables.

The ink jet samples were prepared by printing solid single-color areas with an Olivetti JP 960 ink jet printer using dye-based model inks with known compositions. The papers were coated papers, intended mainly for conventional printing. The model inks consisted of 4 wt.% azo dye, 20 wt.% 2-pyrrolidone and 76 wt.% distilled water. The prints were exposed to artificial sunlight for 6 - 100 h with a Suntest CPS+ xenon arc lamp equipped with an optical filter system, which cuts off the wavelengths below 310 nm. Test chamber settings were 615 Wm^{-2} for irradiance and 40°C for black standard temperature (BST) in every test. According to the data on test chamber conditions, the test chamber temperature (CST) remained fairly constant throughout the exposure periods, but the BST tended to rise towards the end of the runs. Relative humidity, temperature and the composition of air pollutants in the test chamber cannot be adjusted in this test set-up. Hence, they are determined by the predominating conditions of the measurement room (RH 35%, temperature 24°C). Color difference ΔE^* is used as a measure of light fastness, so L*a*b* values were measured from the unprinted papers and prints with a Minolta CM–1000 spectrophotometer before and after light exposure.

In the electrophotographic print studies, two different paper series were used to explore the applicability of the spectroscopic methods. The first series included uncoated and pigmented papers from 80 to 100 gm^{-2}. Another series included coated papers with different

coating compositions. Solid yellow areas were printed with Lexmark Optra C and OKIPage 8 printers. Unfused samples were fixed with a separate Optra C hot roller fuser. The fusing temperatures were varied from 140 to 200°C. Raman and FTIR spectra were measured from toners, unprinted papers and printed samples. To quantify the physical fixing result, toner adhesion was measured with a tape test or with a crease test.

FTIR Spectroscopic Methods

The Bio-Rad FTS 6000 research-grade FTIR spectrometer used in this study has rapid- and step-scan operation capabilities, and is equipped with an attenuated total reflection (ATR) bench, germanium and diamond micro-ATR crystals and a photoacoustic cell (MTEC300). A UMA-500 microscope, equipped with an MCT detector and a CCD video camera, was used in microscopic analyses and computer controlled IR-mapping. In the FTIR-measurements of this study, a sampling resolution of 8 cm^{-1} was used.

The FTIR spectra of the aqueous ink jet inks were measured from dried samples with rapid-scan PAS, since water peaks badly interfere with the interpretation of the IR spectrum. Rapid-scan FTIR-PAS was also used to record the spectra from the toners since with this method the measurement can be made straight from the untreated toner powder.

Unprinted papers and printed samples were measured with the micro-ATR technique, because it is suitable for flexible and reflective surfaces like paper, and its small size enables good contact with the sample. In the ATR method, the penetration depth d_p of the IR beam into the coating depends on the wavelength λ, the angle of the incident light beam α, the refractive indices of the ATR crystal n_1 and the sample material n_2, according to the formula presented in Eq. 1[37].

$$d_p = \frac{\lambda}{4\pi\sqrt{n_1^2 \sin^2 \alpha - n_2^2}} \quad (1)$$

In the case of a diamond crystal, n_1 = 2.4 and α = 45°, so the penetration depth d_p of the IR beam into the coating varies between 0.2 and 1.4 μm, if it is assumed that the refractive index of the sample n_2 = 1.55 (pigment coating). Similarly, in the case of a germanium crystal, n_1 = 4.0 and α = 30°, so the penetration depth d_p of the IR beam varies between 0.18 and 1.0 μm. In addition, the variation of the contact between the crystal and the sample surface affects the penetration depth. To improve the reproducibility of this method, several parallel measurements were made from each sample and the spectra were averaged. The downside of ATR in paper and print studies is the poor spectral resolution from strongly absorbing surfaces. This holds true e.g., for a silica pigment whose bands may dominate the spectra overlapping other peaks. However, spectral subtraction can be used in data analysis to compensate for this. Paper and print samples containing materials with high absorptivity can be measured better with PAS.

ATR mapping was accomplished by using a computer-controlled microscope stage. With this method the measurement steps in the lateral direction can be determined at the desired resolution. Spectral maps of the sample surfaces can be acquired automatically.

In IR spectroscopy, depth profiling of paper and print samples can be accomplished with the step-scan PAS method. In step-scan spectrometers, the mirror is oscillated rapidly around a series of positions along the mirror path. This enables determination of the phase of the PAS signal relative to the infrared beam. The phase of the signal gives information on the probing depth. The phase is determined by measuring the signal through two channels simultaneously: in-phase, I, and in-quadrature, Q. With the phase resolution technique, the phase angle for each point in the spectrum can be calculated using Eq. 2. The phase spectrum is usually displayed with the magnitude spectrum, M, which is a combination of in-phase and in-quadrature spectra (Eq. 3).[38]

$$\theta = \tan^{-1}\left[\frac{Q}{I}\right] \quad (2)$$

$$M = \sqrt{I^2 + Q^2} \quad (3)$$

The depth profiling of the samples is done by altering the modulation frequency of the mirror. At low frequencies, the radiation penetrates deeper into the sample, whereas at higher frequencies it is possible to study the surface layers. In these studies, a series of modulation frequencies ranging from 100 Hz to 900 Hz was used. Thus, the spectrum measured at the fundamental frequency 100 Hz represents the deepest probing depth, whereas the highest harmonics (900 Hz) corresponds to the shallowest probing depth (the surface layers of the print).

Raman Spectroscopic Methods

In this study, two different Raman spectrometers were used. The dispersive Raman spectrometer Kaiser Raman Hololab series 5000 is equipped with a 785 nm laser and an Olympus microscope. This set-up enables microscopic analyses, Raman mapping and confocal depth profiling measurements. Depth profiling can be accomplished at controlled steps, ranging from 0.1 to 10 μm. In the present study, the spectral resolution was 4 cm^{-1}, depth resolution 1 μm and lateral resolution 2.5 μm. To measure larger areas without losing the depth resolution, the sample stage was moved in the x-direction during the measurement to collect an average Raman spectrum from the desired area.

The UV Resonance Raman spectrometer (UVRRS) is a Renishaw 1000 UV, equipped with a Leica-microscope and an Innova 300C FreDTM frequency doubled Ar^+ laser, which can be operated at three different wavelengths (229, 244 and 257 nm). A CCD camera was used for detecting the scattered light. In this study, the laser was operated at a wavelength of 244 nm using an objective with 15x magnification and a resolution of 7 cm^{-1}. Samples were rotated during the collection of spectra to prevent burning of the samples.

Raman spectra of the inks were measured in liquid state and the toner spectra both in powder and in melted state with a 100x dry objective. Raman spectra of unprinted and printed samples were measured with the confocal method using a 100x immersion objective. This method was chosen to be able to quench the fluorescence originating from highly scattering samples like paper pigments. The method is described in more detail in reference[17]. However, fluorescence was found to complicate Raman-measurements and interpretation of the spectra of some colorants and papers, since it significantly lowered the S/N-ratio.

The FTIR and Raman spectroscopic measurement schemes used in this study are summarized in Table I.

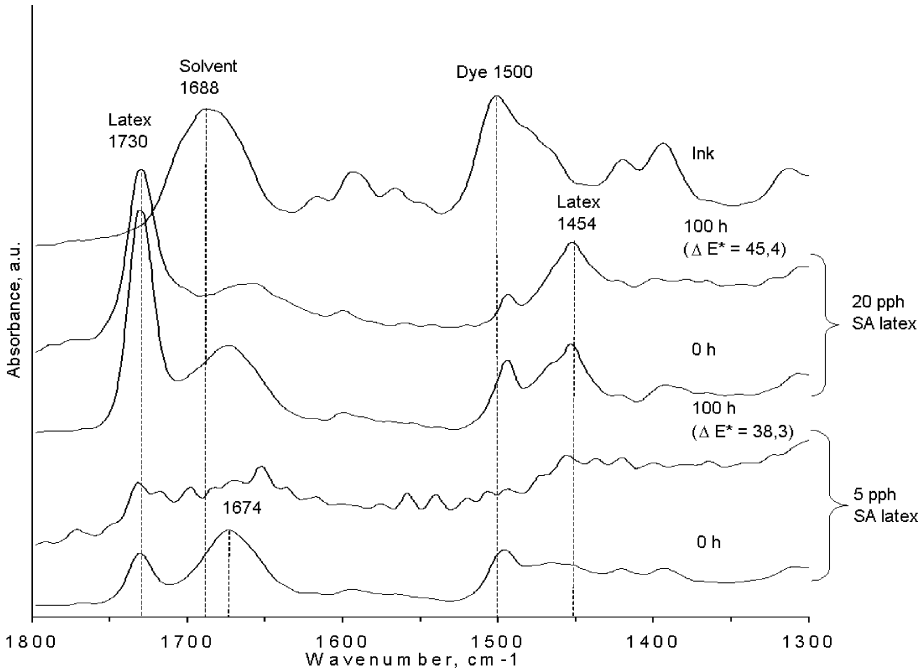

Figure 1. FTIR spectra of dried magenta ink and magenta ink jet prints on kaolin coating before and after 100 h light exposure. SA denotes styrene acrylate. The spectra are shifted vertically for clarity.

TABLE I. FTIR and Raman Spectroscopic Measurement Schemes Used in the Print Studies.

Method	Surface analysis	Depth profiling	Bulk analysis
FTIR	Micro ATR ATR mapping	Step-scan PAS	Rapid-scan PAS
Raman	Confocal Raman UVRRS	Confocal Raman	

Results and Discussion

Ink Jet Print Studies

Surface Measurements. FTIR spectra from surfaces of ink jet prints were measured with a diamond ATR crystal. Figure 1 illustrates the effect of 100 h light exposure on FTIR-ATR spectra of magenta ink jet prints on kaolin-coated papers in which the styrene acrylate latex (SA) content is used as a variable. In addition, an FTIR rapid-scan PAS spectrum of dried magenta ink is also shown.

As is evident from Fig. 1 the most prominent bands in the FTIR-ATR spectra of the printed samples originate from SA latex and ink solvent 2-pyrrolidone. In contrast, the magenta dye can be detected rather poorly from the coating surface, despite of its distinct bands in the wavenumber region 1600-1300 cm^{-1}. The likely reason for this is the behavior of dye-based ink jet inks on the surface of the papers—they do not generally form a separate layer on the paper surface. Rather, a soluble colorant penetrates deeper into the coating with the ink solvents, which complicates its detection. Some remarks can nevertheless be made based on the spectra. As a result of printing, the wavenumber of the ink solvent band originating from carbonyl group[12] decreases from 1688 cm^{-1} to 1674 cm^{-1} (the spectra of 5 pph SA latex 0 h and 20 pph SA latex 0 h). This could indicate the presence of hydrogen bonds between the ink solvent and coating. Similarly, as a result of printing, the dye band at 1500 cm^{-1} shifts to the wavenumber 1495 cm^{-1}, which suggests interaction between the dye and the coating. As a result of 100 h light exposure, both solvent and dye bands decrease in intensity. The extenuation of the ink bands is more extensive on the 5 pph SA latex coating than on 20 pph SA latex coating, which could indicate that the ink has decomposed more on the 5 pph latex coating as a result of light exposure. This is in accordance with the color difference values ΔE^* marked in the figure.

In contrast to the FTIR-methods, Raman-spectroscopy allows easy detection of colorants. Figure 2 presents a part of the Raman spectra of unprinted and unexposed coated paper and of yellow prints exposed to different amounts of light energy. The coating consists of kaolin, with PVA as binder and CMC as dispersant. According to Fig. 2 the spectrum of unprinted coated paper contains only few weak bands in the illustrated wavenumber region. In contrast, the spectra of printed samples contain numerous bands originating from the azo dye.[39] Of these bands, the most prominent ones are the N=N stretching of the azo bond at 1398 cm^{-1} and the C–N stretching between the azo group and adjacent aromatic ring at 1106 cm^{-1}. Generally speaking, extension of the light exposure time results in a decrease in the intensities of dye-originating Raman bands, which suggests the decomposition of the dye. This behavior is in unison with the Δb^* values depicting a change in the yellowness of the prints as a result of light exposure.

In addition to conventional Raman spectroscopy (785 nm laser), preliminary testing of UV Resonance Raman spectroscopy (UVRRS, 244 nm laser) was also carried out, as it was expected that this method could give information on the effect of light exposure on the structures of ink jet colorants. These typically contain aromatic structures and numerous double bonds, which are known to contribute to photodegradation reactions. In addition to this, many coating components contain chemical structures that are sensitive to light.[40] Figure

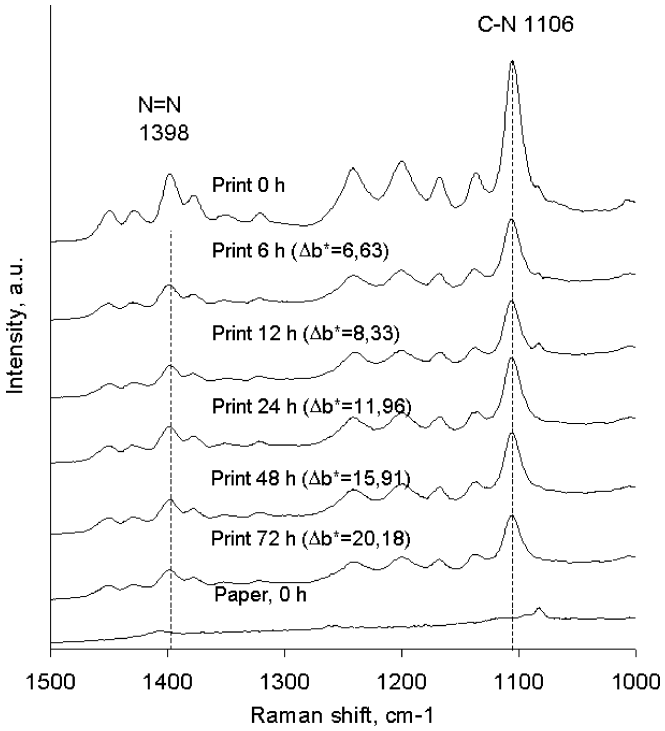

Figure 2. Effect of light exposure time on Raman spectra of yellow ink jet prints. The spectra are vertically shifted for clarity.

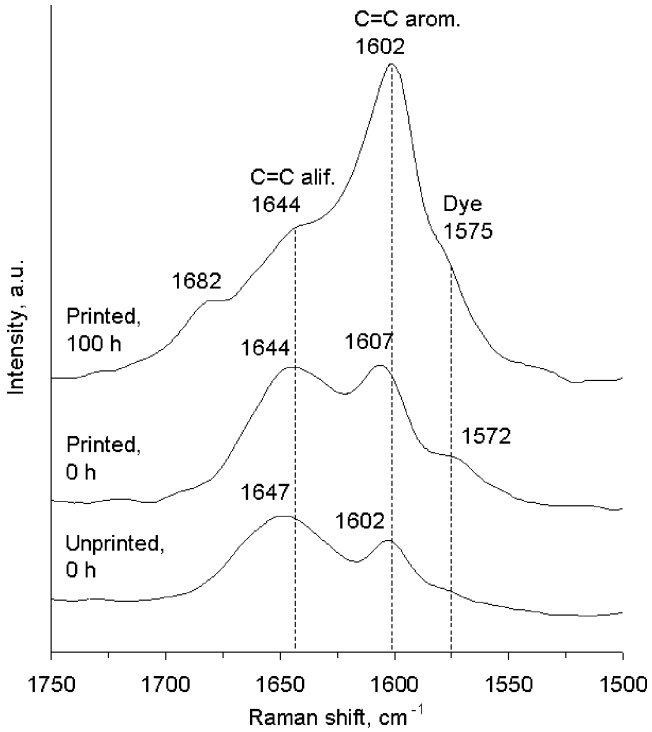

Figure 3. Effect of light exposure on UVRRS spectra of yellow ink jet prints. The spectra are vertically shifted for clarity.

3 presents the 1750 - 1500 cm^{-1} region of the UVRRS spectra of unprinted samples and yellow prints treated with different amounts of light energy. Bands originating from various double bonds typically occur in this wavenumber region.[12] The coating consists of $CaCO_3$ and SB latex. The spectra were scaled to $CaCO_3$ band[12] at 1087 cm^{-1}, since calcium carbonate was expected to remain unchanged in printing and in light exposure.

In the spectrum of the unprinted paper, two prominent bands appear at wavenumbers 1647 and 1602 cm^{-1}, and also a very weak band at 1572 cm^{-1}; see Fig. 3. These likely originate from the various C=C stretching modes[12] of the SB latex. As a result of printing, the band at 1602 cm^{-1} increases and is shifted to 1607 cm^{-1}, and the band at 1572 cm^{-1} intensifies. This suggests interactions between the colorant and the coating. Light exposure for 100 hours results in marked changes in the UVRRS spectrum of the yellow print. The intensity of the band at 1644 cm^{-1} decreases and a new band can be detected at the wavenumber 1682 cm^{-1}. In addition, the band at 1607 cm^{-1} shifts to wavenumber 1602 cm^{-1}, and the dye band at 1572 cm^{-1} to the wavenumber 1575 cm^{-1}. These spectral changes suggest alterationss in the chemical compositions of both the dye and the latex.

Depth Profiling. Depth profiling of ink jet prints gives information on the distributions of ink and paper components, and on possible changes in interactions between them as a result light fading. In this study, depth profiling of ink jet prints was accomplished with FTIR step-scan

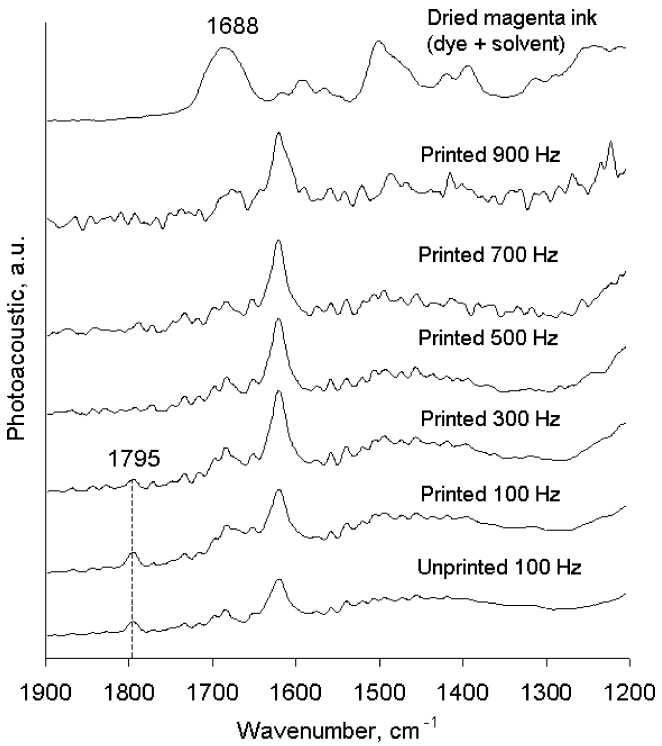

Figure 4. FTIR PAS spectra of unprinted and printed coated papers and dried magenta ink. The spectra are vertically shifted for clarity.

PAS and with the Confocal Raman Method

Figure 4 presents the wavenumber region 1900–1200 cm^{-1} of FTIR step-scan PAS spectra of coated papers before and after printing with magenta ink, and a FTIR rapid-scan PAS spectrum of dried magenta ink. The coated papers in this example are double-coated, with the precoating pigment being $CaCO_3$ and the second coating

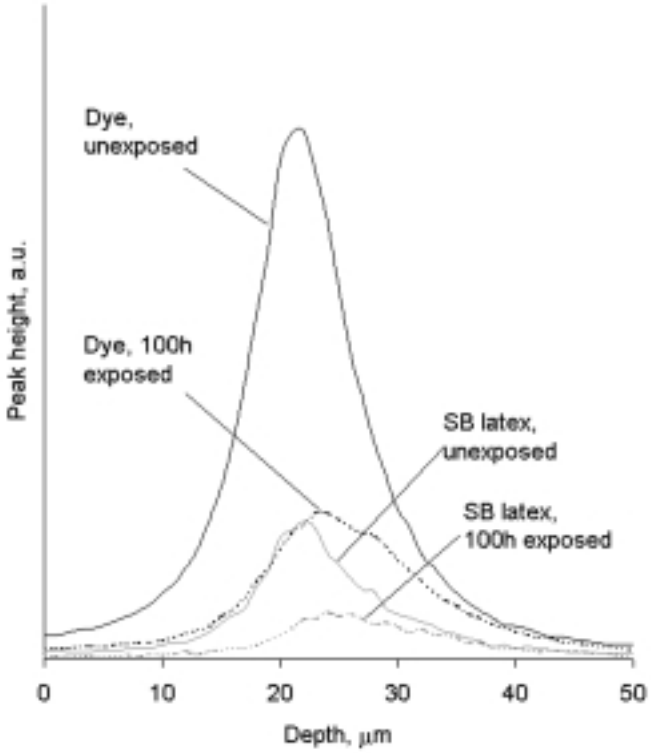

Figure 5. Dye and SB latex distributions in a magenta print before and after light exposure. Solid lines denote untreated prints and dotted lines light-exposed prints.

layer consisting of kaolin, co pigment and SB-latex. All step-scan PAS measurements were accomplished using 100 Hz modulation frequencies, whereas in the rapid-scan measurements, 10 kHz mirror velocity was used. It is evident that the band at 1795 cm^{-1} originating from $CaCO_3$[12] appears in the step-scan PAS spectra measured at the frequencies 100 Hz and 300 Hz. This indicates that the IR beam has penetrated into the interface of the precoating and second coating layers. All the harmonics of the printed samples seem to contain mainly bands from the coating components, with the dye bands being barely visible. This is likely due to the small amount of colorant in the coating layer. In addition, the PAS signals of the highest harmonics, representing the topmost surface layers of the coating, are quite weak and the spectra contain a lot of noise. Thus, these are not useful for spectral interpretation.

Depth profiling of the ink jet prints was also accomplished with the confocal Raman method. Figure 5 shows an example of confocal Raman depth profiles of magenta ink jet prints. The coating consisted of kaolin, co pigment and SB latex. Unexposed and light-exposed distributions were scaled to the pigment band. The profiles of the magenta ink were calculated by following the height of the dye band at 1271 cm^{-1}. It is evident that the dye decomposes from the surface layers of the coating as a result of light exposure. This is seen as a decrease in the intensity of the dye profile and as a shift in its maximum deeper into the coating. This behavior can also be observed for the SB latex, whose Raman depth profile was calculated following the height of the styrene band at the wavenumber 999 cm^{-1} originating from the aromatic rings in the styrene units.[12] The Raman depth profiles thus suggest that both the dye and the latex degrade as a result of light exposure.

Discussion

In light fastness experiments, the most extensive exposure of the samples is usually directed towards the surface layers of the coating. Therefore, detailed analysis of the topmost layers of the print is important. This can be accomplished by combining information from surface analysis and depth profiling spectroscopic measurements.

The advantage of the FTIR methods in ink jet print studies are their suitability for measuring all kinds of coatings without the fluorescence problems often associated with Raman spectroscopy. In addition, they enable characterization of hydrogen bonding between ink and paper components. However, it was found to be rather difficult to detect printed soluble dyes with FTIR from the coating both in surface measurements and in depth profiling, which complicated the interaction analysis. Nevertheless, FTIR methods allow printed dyes to be studied, even though the dye bands are not distinct, if spectral subtraction is used. This may nonetheless be a tedious procedure, especially in depth profiling.

In contrast to the FTIR methods, both of the tested Raman measurements were sensitive to even very small amounts of the printed soluble ink jet dyes used in this study and to the light-induced changes in them. Seen in the light of the preliminary results, UV Resonance Raman spectroscopy appears to be a particularly promising method for photo-degradation studies of ink jet prints because of its sensitivity to double bonds. The main difficulty of the Raman measurements is the extensive fluorescence of certain compounds. For example, most ink jet colorants and coating pigments give rise to a strong fluorescence that complicates interpretation of the spectra. This behavior could be alleviated to some extent by using the immersion objective in the confocal Raman measurement. Therefore, a reasonable comparison of different samples could be made by normalizing the spectra to some common compound in the samples with known content and by calculating the depth profiles based on the peak height rather than the area. In addition to the obtrusive fluorescence, the Raman spectra of all CMYK colors could not be collected using similar measurement conditions. For example, cyan and black dyes tended to burn up during the Raman measurement, whereas yellow and magenta could be measured without problems. This is most likely due to the fact that both cyan and black absorb light at long wavelengths, and the laser wavelength used in this Raman test set-up was 785 nm. Thus, strong absorption of energetic monochromatic light may cause overheating of the printed sample and eventually lead to combustion. Adjustment of the laser wavelength may help to restrain both the combustion of dark colors and the fluorescence, at least partially.

The most facile depth profiling method for the ink jet prints proved to be confocal Raman spectroscopy. This is mainly due to its sensitivity to the chemical structures typical of ink jet colorants. In addition, the test set-up used in this study allows controlled movement of the sample stage and therefore the exact probing depth at each point is known. In FTIR step-scan PAS the probing depth depends on the thermal diffusivity of the coating and on the modulation frequency. The determination of the exact penetration depth of the IR beam into the sample therefore requires information on the thermal diffusivities of the coating components. This makes the analysis of depth profiling results of composite structures like coatings and the samples containing unknown components rather complicated. Another drawback of depth profiling with FTIR step-scan PAS was the rather

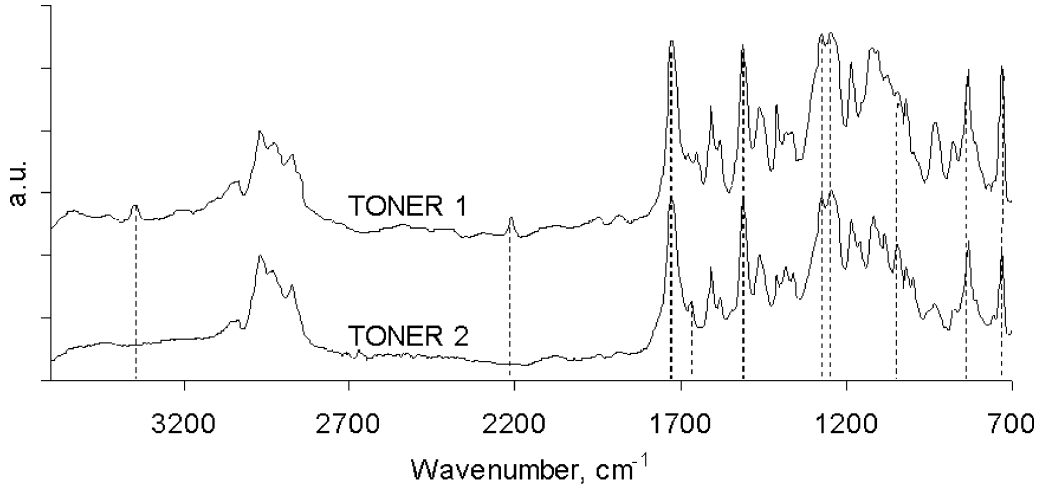

Figure 6. FTIR PAS spectra of polyester resin toners. The spectra are vertically shifted for clarity.

long measurement time compared to confocal Raman. An increase in the modulation frequency speeds up the measurement and also probes the coating closer to the surface, which facilitates the detection of the colorant. However, the exact penetration depth of the IR beam still remains unknown. In addition, the S/N ratios of the spectra tend to decrease as a result of increased modulation frequency.

Electrophotographic Print Studies

Toner Identification. The FTIR rapid-scan PAS and Raman spectroscopic methods together proved to be a powerful tool in identifying the composition of the toners. Since the toners mainly consist of polymer resins, the FTIR method is particularly suitable for the chemical analysis. There is great complexity in the spectra obtained from the toner due to the existence of overlapped bands, changes in their shapes and displacements along the frequency axis. Otherwise, the spectra were relatively clean, implying an absence of notable noise after an adequate number of parallel scans.

In both methods, the measurement could be made straight from the toner powder, without any pre-processing. In some of the Raman measurements, scattering from the powder sample impaired the quality of the spectra. Parallel measurements eliminated this effect. To reduce the number of parallel scans, measurements from the melted toners were also tried. As a result, identical Raman spectra were obtained from the un-melted and melted toners. In the FTIR measurements, the color of the toner had no relevance for the measurement, whereas in the Raman measurements, the power of the laser had to be adjusted in relation to the darkness, and hence the absorptivity of the toner powder. For this reason, the yellow toner with the lowest light absorption levels was chosen for these experiments. In these experiments, there was no noticeable fluorescence, which is known to occur frequently in Raman measurements.

Raman measurements from the toners show distinct bands for the toner pigment, whereas with FTIR, mainly bands for the toner resin are detected. This was established reliably because the composition of toner **1** was known and peaks in the spectra could therefore be assigned easily. Toner **1** consists of a polyester resin and an acetamide pigment. The polyester resin in question has five components: two bisphenol A derivatives, an aromatic acid and two different polycarboxylic acid anhydrides. From the FTIR spectra of toner powders, illustrated in Fig. 6, it is clear that toner **2** consists of a similar polyester resin. The significant peaks of the toner powders measured with FTIR rapid-scan PAS are marked in Fig. 6 and the corresponding peak assignments are shown in Table II. The peak assignments are based on various reference books of vibrational spectroscopy[12,37,41] and on previous studies of resins[42] and latexes.[27,35]

TABLE II. Peak Assignments for the Polyester Toners. Symbols: υ Stretching Vibration, δ Deformation Vibration, ϕ Aromatic Ring.[12,27,37,41,42]

Tentative Assignment	Toner 1 Band position (cm^{-1})	Toner 2 Band position (cm^{-1})
OH, υ	3426.6	3428.4
NH, υ	3344.7	-
CN, υ	2212.7	-
C = O, υ	1725.3	1725.4
C = N, υ	-	1667.4
C = C ϕ, υ	1511.3	1510.4
C-O + C-C, υ	1273.4	1272.4
ϕ-O, υ	1246.7	1246.1
ϕ-O-C, υ	1047.0	1046.1
ϕ-H, δ out of plane	832.1	830.9
ϕ-H, wag	731.5	731.9

The only significant differences between the two toners arise from the yellow pigments. The pigment in toner **1** is an acetamide, shown by the C-N and N-H stretching vibrations at 2212 cm^{-1} and 2245 cm^{-1}, respectively. The pigment in toner **2** can be defined to be an azo pigment based on the peak 1667 cm^{-1} (C = N stretching vibration). Raman measurements from toner **2** support this finding, as the azo bond N = N at 1395 cm^{-1} and C-C bond of aromatic structures at 1598 cm^{-1} are clearly visible.

Depth Profiling of the Electrophotographic Prints. One of the main advantages in using the FTIR methods to study electrophotographic prints is the possibility of making measurements from different depths in the sample. FTIR spectra were measured from the yellow prints with the step-scan PAS cell and two ATR crystals to obtain spectral data from seven different depths in the print sample. The measurement point nearest to the

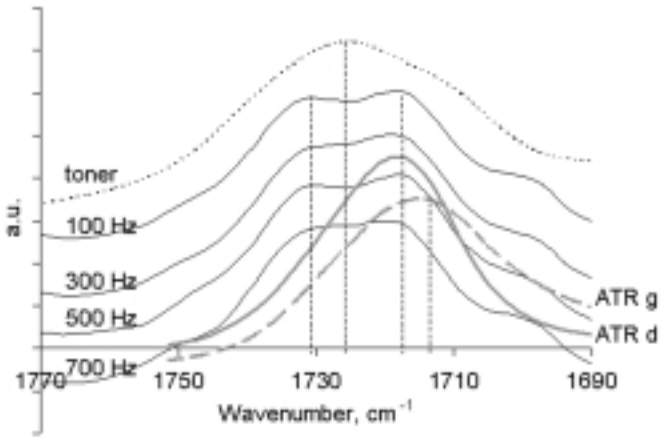

Figure 7. Shifts of C = O peak position on a coated paper sample. The spectra are vertically shifted for clarity.

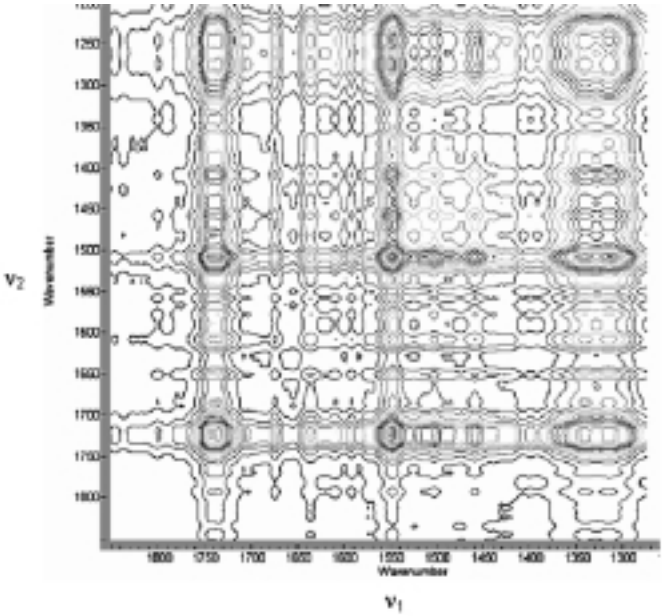

Figure 8. 2D correlation spectrum of a yellow print on a calendered paper sample.

surface is achieved with the ATR germanium crystal (g). The measurement depth with the ATR diamond crystal (d) is a few micrometers deeper from the previous point. In the step-scan PAS measurement, the depth increases as the modulation frequency decreases. In these measurements five different frequencies were used, from 900 to 100Hz in decreasing order. For polymeric samples this means depths from 6 to 13 μm, respectively. The spectra could be measured from untreated print samples in both methods. This is very important and a great advantage, since any pretreatment could have a significant effect on the quality of the spectra. Overlapping peaks from the possible pretreatment substance could also disturb the detection of the significant peak of the sample. It is also possible to use the same sample for further chemical or optical analysis after the FTIR measurement.

There were specific regions in the spectra where differences between the depths were found. In general, peaks from the papers were clearly seen deeper in the sample (at 100 Hz) but they were not visible in the surface. This is to be expected because the toner layer is fairly thick. The measurement depth in the ATR measurements is only a few micrometers and so the ATR spectra contain only peaks from the toner resin. If the changes in the chemical structure of the toner resin are to be examined, relevant regions in the spectra are the carboxyl stretching region around 3700-3300 cm^{-1}, the carbonyl stretching region around 1725 cm^{-1} and the C-O-C region of the ester around 1280-1240 cm^{-1}.

Figure 7 shows an example of the carbonyl peak position of a toner layer printed on one of the coated paper samples with toner **1**. The figure illustrates the effect of the measurement depth on the position of the carbonyl stretching band (C=O). When the carbonyl band (1725 cm^{-1}) measured from the toner powder is compared with the spectra measured from the prints with step-scan PAS at different depths, a peak splitting is detected. It is noted that as the focusing depth decreases, the intensity of the carbonyl band at 1719 cm^{-1} increases in relation to the band at 1730 cm^{-1}. This increase may indicate an increase in the concentration of a distinct component of the polyester towards the surface of the toner layer. When spectral data from the ATR measurements are compared with those of the step-scan PAS, it can be seen that the peak around 1730 cm^{-1} disappears. Also, a shift from 1719 to 1715 cm^{-1} is noted when diamond and germanium crystal data are compared, respectively. The splitting of the carbonyl peak, illustrated in Fig. 7, could originate from stratification processes of individual components in the sample[35] or from hydrogen bonding, since it is known that frequency shifts, band broadening and intensity changes in the carbonyl and hydroxyl bands of ester and alcohol groups of the polymers manifest hydrogen bonding.[41]

The use of the 2D correlation method has simplified the analysis of the spectral data from the step-scan PAS measurements. A 2D correlation spectrum of a collection of spectra at different depths gives information on the locations of the peaks in the spatial axis in relation to each other. Figure 8 illustrates a synchronous 2D correlation spectrum of the region of 1800 – 1200 cm^{-1} measured from the same print sample as in Fig. 7. In 2D correlation spectra, a positive wavenumber ratio (ν_1/ν_2) means that the peak in ν_1 (x-axis) is located deeper in the sample than the peak in ν_2 (y-axis). Correspondingly, a negative contour means that ν_1 is shallower than ν_2.[43] Positive contours are indicated in Fig. 8 with light areas and negative ones with dark areas. It can be seen that there is a positive contour at 1730/1719 cm^{-1}, indicating that the origin of band 1730 is deeper than that of 1719 cm^{-1}. This verifies the results shown earlier. There is a similar effect in the C-O-C region of ester (~1250 cm^{-1}) and aromatic ring region (~1500 cm^{-1}).

Another depth profiling method was also used to extend the perspective. Confocal Raman measurements were made from solid yellow prints. In the confocal Raman measurements the samples have to be treated with an immersion oil[17] but this was found not to have a significant effect on the interpretation of the spectra due to the careful choice of the oil. With this method it is possible to obtain a more exact depth profile of the sample, since the exact measurement steps and depth can be set in the control program. A downside of the electrophotographic samples is the fact that the peaks from the toner pigment dominate and the peaks from the resin are not properly detected. Nevertheless, the location of the toner pigment gives information on the toner's composition in relation to the paper and on the thickness of the toner layer.

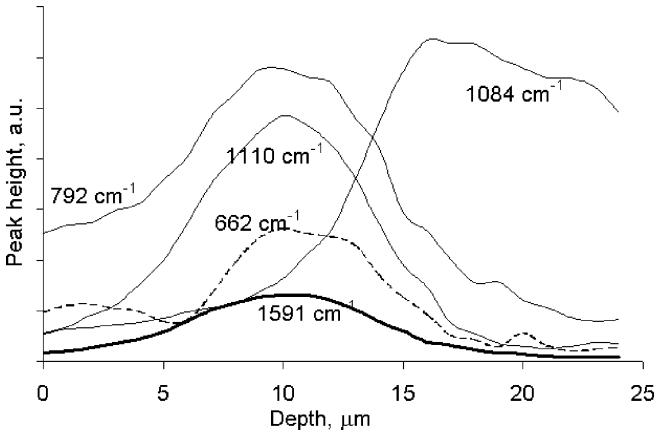

Figure 9. Confocal Raman spectrum of a calendered sample.

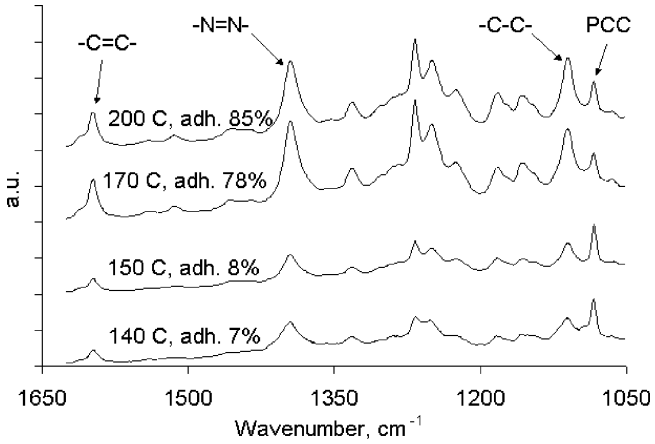

Figure 10. Part of confocal Raman spectra at the toner maximum at fixing temperatures 140, 150, 160 and 170°C. The spectra are vertically shifted for clarity.

When the spectra measured from a print at different depths are compared, a transition phase from the maximum concentration of toner to the maximum intensity region of paper components can be defined. It is clear that while going deeper into the sample, bands characteristic of the paper components emerge, while bands from the toner diminish. Figure 9 illustrates the peak heights of given assigned bands of Raman spectrum of toner **1** at different depths in the sample. As was already mentioned, the bands in the Raman spectrum arise mainly from the toner pigment, which in this case was an acetamide. The four peak intensity profiles on the left side of Fig. 9 may be assigned[12,17] to the pigment as follows: NH deformations (1591 cm^{-1}), aromatic ring vibrations (662 and 1110 cm^{-1}) and CH deformations (792 cm^{-1}). The intensity profile of the peak at 1084 cm^{-1} arises from the $CaCO_3$ in the paper.[17] It can clearly be seen that the toner forms a fairly compact layer, which starts to intermingle with the paper at around 12 μm. At 16 μm depth the paper peak reaches a maximum and at this point there is only a fraction of toner left. The interfacial region is approximately 8 μm wide.

Figure 10 presents parts of confocal Raman spectra at maximum toner concentration at different fixing temperatures. It can be noted that toner bands from the yellow azo pigment (Toner **2**: N=N bond in yellow azo pigment at 1395 cm^{-1} and C-C bond in aromatic structures at 1598 cm^{-1})[12] strengthen in relation to the PCC band (1084 cm^{-1})[17] as the fixing temperature increases. The adhesion levels measured with a tape test (labeled in Fig. 10) increase as a function of the fixing temperature. When given toner bands were scaled to the reference (cellulose band at 376 cm^{-1}),[17] there was a linear correlation with the obtained intensity ratios and the measured toner adhesion. This could indicate that the improved toner adhesion is also reflected in changes in the toner pigment peak intensities, although the resin part is mainly involved in the fixing of the toner.

Analysis of the Surface. The previous examples have shown that the composition and structure of the toner layer in the spatial direction can be analyzed with vibrational spectroscopic methods using different kinds of detection methods. The composition of the toner layer can also be observed in the lateral direction. The surface formation can best be investigated with μ-ATR mapping. Because the toner layer is fairly thick, covering and uniform, the surface measurement of a compact area shows only information on the toner resin and the use of a mapping option is redundant. Mapping was therefore used to investigate the treated surfaces, for example adhesion-tested sample areas.

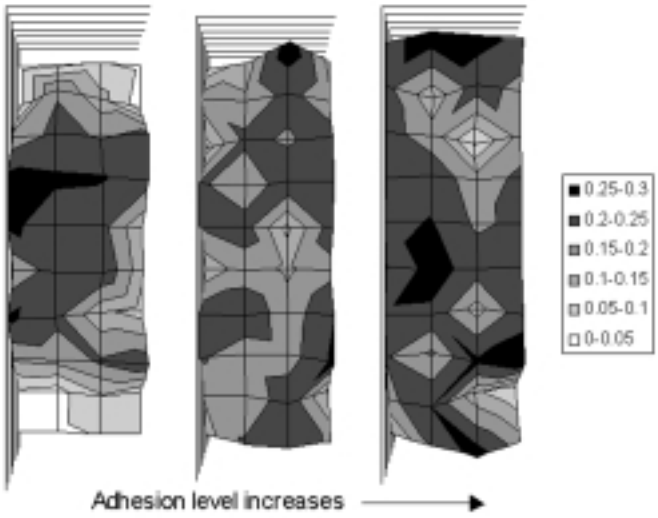

Figure 11. X,Y-map of a print surface after tape test. The numerical values in the legend denote peak intensities.

ATR maps were made of surfaces of three samples fixed at three different fixing temperatures from the area where the adhesion tape test was performed. Figure 11 illustrates the carbonyl peak intensity deviation in the affected region. The maps of the surfaces show that as the adhesion increases, the carbonyl peak intensity increases (darker areas). Also, in the more adhered interfaces the average intensity is higher. In those surfaces, no areas where all the toner had come out as a result of the tape test were observed. This supports the visual observation.

Conclusions

The goal of this study was to evaluate the applicability of vibrational spectroscopic methods to the study of digital prints. The variables of the light fading experiments

in ink jet and fixing experiments in electrophotography cause systematic spectral changes in FTIR and Raman spectra.

In the case of ink jet prints, both Raman and FTIR spectroscopy appear to be applicable to studying paper–ink interactions, since changes in the spectra due to light exposure could be observed. Especially UV Resonance Raman spectroscopy seems to be a very promising method for photo-degradation studies of ink jet prints. Of the depth profiling methods studied here, confocal Raman spectroscopy proved to be more suitable for studying the light fastness of dye-based ink jet prints than FTIR step-scan PAS. This is mainly due to the sensitivity of Raman spectroscopy to the chemical structures of ink jet colorants, the good S/N ratio of the spectra obtained from the topmost surface layers of the print and the knowledge on the exact probing depth.

In studying electrophotographic prints, Raman and FTIR spectroscopic methods proved to give complementary information as was to be expected based on the theories. The Raman method is sensitive to the toner pigments, whereas different FTIR detection methods are sensitive to the toner resin. The two depth profiling methods seem especially suitable for examining toner-paper interactions. With the step-scan PAS method it is possible to detect the interfacial region of the toner and paper. For example hydrogen bonding induced by the fixing process may be detected in the toner layer. With the confocal Raman method it is possible to study the composition of the toner layer further. The distribution of the toner pigment may for instance be indicated as a function of the exact depth of the toner layer. The use of the 2D correlation method associated with the step-scan PAS method and the mapping option with the micro-ATR method may provide additional information. ▲

Acknowledgment. We would like to thank Professor Pirkko Oittinen of the Laboratory of Media Technology at the Helsinki University of Technology for her input as a supervisor of this study. Financial support from the Technology Development Center of Finland (TEKES) and from the International Ph.D. Programme in Pulp and Paper Science and Technology (PaPSaT) is also gratefully acknowledged.

References

1. L. Shaw-Klein, in *Proc. IS&T's NIP14 Conference*. IS&T, Springfield, VA, 1998, pp. 129–132.
2. D. Juhué and J. Lang, *Langmuir* **9**, 792 (1993).
3. A. Stübbe, A. Karl, and W. Kalbitz, in *Proc. IS&T's NIP14 Conference,* IS&T, Springfield, VA 1998, pp. 103-106.
4. J. F. Oliver and L. Kale, in *Proc. TAPPI Papermakers Conference 1985*, pp. 217-222.
5. D. W. Donigian, P. C. Wernett, M. G. McFadden, and J. J. McKay, *Tappi J.* **8**, 175 (1999).
6. S. J. Sargeant, T. Chen and B. Parikh, in *Proc. IS&T's NIP14 Conference,* IS&T, Springfield, VA, 1998, pp. 138–141.
7. H. Oka and A. Kimura, *J. Imaging Sci. Technol*. **39**, 239 (1995).
8. M. M. Farrow, A. G. Miller and A. M Walsh, in *Colloids and Surfaces in Reprographic Technology*, ACS, Washington D.C., 1982, pp. 455–474.
9. U. P. Agarwal and R. H. Atalla, in *Surface Analysis of Paper*, CRC Press, USA, 1995, pp. 152–181.
10. K. Vikman, K. Sipi and P. Oittinen, in *Proc. IS&T's NIP16 Conference,* IS&T, Springfield, VA, 2000, pp. 408–413.
11. K. M. Sipi, in *Proc. IS&T's NIP17 Conference,* IS&T, Springfield, VA, 2001, pp. 145-150.
12. D. Lin-Vien, N. B. Colthup, W. G. Fateley, and J. G. Grasselli, *The handbook of infrared and Raman characteristic frequencies of organic molecules,* Academic Press, New York, 1991. p. 503.
13. P. L. Lang, J. Cook, B. Fuller, M. Scott, C. S. Telles, and T. Barrett, *Appl. Spectr*. **52**, 713 (1998).
14. A. Kher, M. Mulholland, B. Reedy, and P. Maynard, *Appl. Spectr*. **55**, 1192 (2001).
15. M. Halttunen, J. Tenhunen, T. Saarinen, and P. Stenius, *Vibr. Spectr.* **19**, 261 (1999).
16. E. Kenttä, K. Juvonen, M. Halttunen, and J. Vyörykkä, *Nord. Pulp Pap. Res. J.* **15**, 579 (2000).
17. J. Vyörykkä, M. Halttunen, H. Iitti, E. Kenttä, J. Paaso, J. Tenhunen, T. Vuorinen, and P. Stenius, in *Proc. 2001 Coating and graphic arts conference and trade fair*, TAPPI Press, Atlanta, GA, 2001, pp 193-201.
18. M. Halttunen, M. Löija, T. Vuorinen, P. Stenius, J. Tenhunen, and E. Kenttä, in *Proc. 2001 Coating and graphic arts conference and trade fair*, TAPPI Press, Atlanta, GA, 2001, pp. 203-211.
19. A. T. Slark and P. M. Hadgett, *Polymer* **39**, 2055 (1998).
20. A. T. Slark and P. M. Hadgett, *Polymer* **40**, 1325 (1999).
21. M. Kaplanová, *J Prepr. Print. Tech.* **2**, 4 (1998).
22. A. P. Kushelevsky and M. A. Slifkin, *J. Oil Colour Chem. Assoc*. **70**, 99 (1987).
23. S. Kokot, N. A Tuan and T. L. Rintoul, *Appl. Spectr.* **51**, 387 (1997).
24. L. A. Lyon, C. D. Keating, A. P. Fox, B. E. Baker, L. He, S. R. Nicewarner, S. P. Mulvaney, and M. J. Natan, *Anal. Chem*. **70**, 341R (1998).
25. S. P. Mulvaney and C. D. Keating, *Anal. Chem*. **72**, 145 (2000).
26. C. Rodger, G. Dent, J. M. Watkinson, and W. E. Smith, *Appl. Spectr.* **54**, 1567 (2000).
27. B-J. Niu and M. W. Urban, *J. Appl. Polym. Sci.* **70**, 1321 (1998).
28. B. Yan and Q. Sun, *J. Org. Chem.* **63**, 55 (1998).
29. S. Hajatdoost and J. Yarwood, *Appl. Spectr*. **50**, 558 (1996).
30. X. Hu and X. Li, *J. Polym. Sci. B* **37**, 965 (1999).
31. S. Higuchi, T. Hamada, and Y. Gohshi, *Appl. Spectr.* **51**, 1218 (1997).
32. F. X. Perrin, M. Irigoyen, E. Aragon, and J. L. Vernet, *Polym. Degr. Stab.* **70**, 469 (2000).
33. A. J. Vreugdenhil, M. S. Donley, N. T. Grebasch, and R. J. Passinault, *Progr. Org. Coat.* **41**, 254 (2001).
34. M. W. Urban and E. M. Salazar-Rojas, *J. Polym. Sci. A* **28**, 1593 (1990).
35. M. W. Urban, C. L. Allison, G. L. Johnson, and F. Di Stefano, *Appl. Spectr.* **53**, 1520 (1999).
36. M. Brogly, M. Nardin and J. Schultz, *Polymer* **39**, 2185 (1998).
37. H. A. Willis, J. H. van der Maas and R. G. J. Miller, Eds., *Laboratory Methods in Vibrational Spectroscopy*, John Wiley and Sons, London, UK, 1987, p. 545.
38. A. Rosencwaig, *Photoacoustics and Photoacoustic Spectroscopy*, Krieger, USA, 1990, p. 309.
39. N. Biswas and S. Umapathy, *J. Phys. Chem. A* **104**, 2734 (2000).
40. I. Forsskåhl, in *Forest Products Chemistry. Papermaking Science and Technology,* Fapet, Helsinki, Finland, 2000, pp. 277–332
41. D. I. Bower and W. F. Maddams, *The Vibrational Spectroscopy of Polymers*. Cambridge University Press, Cambridge, UK, 1989, p. 313.
42. I. Noda, *Appl. Spectr.* **44**, 550 (1990).